

AD-A094 338

VIRGINIA UNIV CHARLOTTESVILLE DEPT OF CHEMISTRY  
ELECTRON-RICH CARBORANES. STUDIES OF A STEREOCHEMICALLY NOVEL S--ETC(U)  
JAN 81 D C FINSTER, R N GRIMES  
N00014-75-C-0305  
NL

UNCLASSIFIED TR-37

1 1  
AD-A094 338

END  
DATE  
FILED  
2 81  
DTIC

AD A094338

OFFICE OF NAVAL RESEARCH

CONTRACT NO. N00014-75-C-0305

12  
LEVEL II

TECHNICAL REPORT NO. 37

14 TR-371

Electron-Rich Carboranes. Studies of a Stereochemically Novel  
System,  $(\text{CH}_3)_4\text{C}_4\text{B}_7\text{H}_9$ , an 11-Vertex Arachno Cluster.

10 David C. Finster and Russell N. Grimes

Department of Chemistry  
University of Virginia  
Charlottesville, Va. 22901

DTIC  
ELECTED  
JAN 30 1981  
S D

Prepared for Publication in

Journal of the American Chemical Society

11 January, 1981

11-47

Reproduction in whole or in part is permitted  
for any purpose of the United States Government

DDC FILE COPY

Approved for public release; distribution unlimited

401147

81 1 30 006

Electron-Rich Carboranes. Studies of a Stereochemically Novel

System,  $(\text{CH}_3)_4\text{C}_4\text{B}_7\text{H}_9$ , an 11-Vertex Arachno Cluster<sup>1</sup>

David C. Finster and Russell N. Grimes\*

Contribution from the Department of Chemistry  
University of Virginia  
Charlottesville, VA 22901

Abstract. The controlled degradation of  $(\text{CH}_3)_4\text{C}_4\text{B}_8\text{H}_8$  (I) in 95% ethanol in air gives  $(\text{CH}_3)_4\text{C}_4\text{B}_7\text{H}_9$  (II). Electrophilic bromination of II produces 11-Br- $(\text{CH}_3)_4\text{C}_4\text{B}_7\text{H}_8$  (III), which is shown in an X-ray diffraction study to have an open cage structure with a bridging  $-\text{CH}(\text{CH}_3)-$  group across the open face; compounds II and III can be described as 11-vertex arachno cages. Deprotonation of II with NaH in THF generates the monoanion  $(\text{CH}_3)_4\text{C}_4\text{B}_7\text{H}_8^-$  (IV) from which the CH proton on the bridging group has been removed. Protonation of IV gives a new isomer of  $(\text{CH}_3)_4\text{C}_4\text{B}_7\text{H}_9$  (V), whose  $^{11}\text{B}$  and  $^1\text{H}$  FT NMR spectra indicate a substantially different cage geometry from that of II. The molecular structures of II-V and pathways for their interconversion are discussed in light of NMR, ir, mass spectroscopic, and X-ray evidence. Crystal data for III:  $\text{BrC}_8\text{B}_7\text{H}_{20}$ ; mol wt 271.84, space group PI,  $z = 2$ ;  $a = 7.764(3)$ ,  $b = 8.352(5)$ ,  $c = 12.317(6)\text{\AA}$ ;  $\alpha = 94.53(5)$ ,  $\beta = 95.41(5)$ ,  $\gamma = 120.51(5)$ ;  $V = 678\text{\AA}^3$ ;  $R = 0.057$  for 1404 independent reflections having  $F_O^{2 > 3\sigma(F_O^2)}$ .

Accession For NTIS DTIC TAB Unpublished Justification	By Distribution/ Availability Codes	Avail and/or Special
<input checked="" type="checkbox"/>	<input checked="" type="checkbox"/>	<input checked="" type="checkbox"/>

The high-yield preparation<sup>2</sup> of the tetracarbon carborane  $(\text{CH}_3)_4\text{C}_4\text{B}_8\text{H}_8$  (I) has opened up new, intriguing avenues in boron cage synthesis, and a variety of 11- to 14-vertex metallacarboranes has been obtained<sup>3</sup> by insertion of transition metals into I, both directly and via the carborane dianion  $(\text{CH}_3)_4\text{C}_4\text{B}_8\text{H}_8^{2-}$ . Compound I is an "electron-rich"<sup>4</sup> nido cage, with 28 skeletal bonding electrons compared to the requirement<sup>5</sup> of 26 for a closo (icosahedral) 12-vertex polyhedron, and consequently adopts a distorted cage geometry; moreover, many of the metallacarboranes derived from I also have unusual, often unique, cage structures.<sup>3,6</sup> Most of our attention has been directed to the structural consequences of metal insertion into I. However, a recent study<sup>7</sup> did examine the introduction of additional electrons to I, forming the 12-vertex, 30-electron  $(\text{CH}_3)_4\text{C}_4\text{B}_8\text{H}_8^{2-}$  dianion which has a more open (arachno) structure than I itself.

Clearly other aspects of the chemistry of I merit attention as well, and in parallel with the properties of the well-known icosahedral  $\text{C}_2\text{B}_{10}\text{H}_{12}$  carboranes,<sup>8</sup> it was of interest to explore the degradation of I to smaller cage systems. The present investigation was concerned with the conversion of I to a  $\text{C}_4\text{B}_7$  species and the quite unexpected stereochemistry which was uncovered in the course of events.

#### Results and Discussion

Cage Degradation of  $(\text{CH}_3)_4\text{C}_4\text{B}_8\text{H}_8$ . The carborane  $(\text{CH}_3)_4\text{C}_4\text{B}_8\text{H}_8$  (I) is a white, air-stable solid, m.p.  $138^\circ\text{C}$ , which is remarkably

volatile at room temperature (in contrast to the  $C_2B_{10}H_{12}$  carboranes, which are essentially nonvolatile).<sup>2</sup> The distorted-icosahedral solid-state structure of I (Figure 1, isomer A) was determined crystallographically several years ago,<sup>9</sup> and recently the cage structural parameters were more precisely established from an X-ray study of the B(4)-ferrocenyl derivative which was shown to have the same framework geometry.<sup>10</sup> In solution, isomer A exists in equilibrium with a second isomer (B, Figure 1) which has not been isolated; on removal of solvent the mixture reverts entirely to A. The geometry depicted for B has been proposed<sup>7</sup> from  $^{11}B$  and  $^1H$  FT NMR observations and by consideration of the known structures of metal complexes derived from I and its dianion. This behavior is very different from that of  $1,2-C_2B_{10}H_{12}$ , which is non-fluxional in solution and isomerizes only above  $400^\circ C$ , and then irreversibly.<sup>8</sup>

In light of the well-known degradation of  $1,2-C_2B_{10}H_{12}$  to  $C_2B_9H_{12}^-$  by the action of Lewis bases,<sup>11a,b</sup> similar behavior was expected for I. Compound I does not react with  $(C_2H_5)_3N$  or tetrahydrofuran (THF) in the absence of air, but it does undergo slow, controlled degradation over several hours in 95% ethanol at room temperature in air, forming a new carborane,  $(CH_3)_4C_4B_7H_9$  (II). Compound II, a white, air-stable solid, m.p. (dec.)  $190^\circ C$ , has been isolated in 40-60% yields. The presence of water is evidently essential in this reaction, since I is unreactive toward dry ethanol or methanol; in 95% aqueous THF in air, I decomposes to uncharacterizable products, as is also the case when I is treated with  $(C_2H_5)_3N$  in air.

The degradation of I can be written as



which is analogous to the conversion of  $\text{C}_2\text{B}_9\text{H}_{11}$  to  $\text{C}_2\text{B}_7\text{H}_{13}^{11c}$ ,

but the actual stoichiometry may be more complex than the equation suggests. Carborane II is identical to a product, previously unreported, which was obtained<sup>12</sup> in low yield in the reaction of  $\text{Na}^+[(\text{CH}_3)_2\text{C}_2\text{B}_4\text{H}_5]^-$  with  $\text{FeCl}_2$  at room temperature (see Experimental Section).

Structural Characterization of II. Compound II was initially formulated as  $(\text{CH}_3)_4\text{C}_4\text{B}_7\text{H}_7$  on the basis of its chemical ionization (CI) and electron impact (EI) mass spectra, which exhibit sharp cutoffs at m/e 193 (M+1) and 192, respectively (Figure 2). Other than small peaks attributable to <sup>13</sup>C-containing ions, there are no significant EI intensities above m/e 192, implying the absence of "extra" (e.g., B-H-B bridging) hydrogen atoms. Nonetheless, subsequent work established that two extra hydrogens are indeed present, and II is in fact  $(\text{CH}_3)_4\text{C}_4\text{B}_7\text{H}_9$  (MW 194). This conclusion was derived from FT NMR and ir spectra of II and its B-bromo derivative (III) (Figures 3 and 4; Tables I-III), the mass spectrum of III (Figure 2), and an X-ray crystal structure determination on III, described below. Hence the low intensities of m/e 193 and 194 peaks in the mass spectra of II are attributed to extremely facile loss of two hydrogen atoms in the heated sources of the spectrometers, such that only the spectra of  $(\text{CH}_3)_4\text{C}_4\text{B}_7\text{H}_7$  are observed. In the bromo derivative, the loss of hydrogen is not complete and the expected parent peaks are, in fact, present.

Bromination of II. Treatment of II with  $\text{Br}_2$  in carbon disulfide solution over  $\text{AlCl}_3$  produced a monobromo derivative,  $(\text{CH}_3)_4\text{C}_4\text{B}_7\text{H}_8\text{Br}$  (III), which was isolated in 50% yield as a colorless,

air-stable solid (m.p. 225°C). From the close similarity of the  $^{11}\text{B}$  and  $^1\text{H}$  FT NMR spectra of II and III (Figures 3 and 4), it is apparent that these species have the same cage geometry and that III is in fact a bromo-substituted derivative of II (see discussion below). The cage structure of III was subsequently established from an X-ray study of III as follows.

Crystal Structure of  $^{11}\text{Br}\text{-}(\text{CH}_3)_4\text{C}_4\text{B}_7\text{H}_8$  (III). The molecular geometry is illustrated in Figures 5 and 6, with relevant data listed in Tables IV-VII. The cage framework consists of an open  $\text{C}_3\text{B}_7$  basket with a "handle" formed by a bridging  $-\text{CH}(\text{CH}_3)-$  group across the opening. The three skeletal carbon atoms occupy vertices on the open rim, and all four nonmethyl carbons retain a contiguous relationship. The bromine atom is attached to  $\text{B}(11)$ , adjacent to the bridging carbon [C(7)], and the two "extra" hydrogens are located on C(7) and in a B-H-B bridge as shown. There are no unusual B-B or B-C bond distances (Table V) but the two framework C-C bonds [C(2)-C(3) and C(7)-C(8)] are relatively long for interactions between low-coordinate skeletal carbon atoms.<sup>13</sup> The bridging hydrogen, H(910) is only 1.99 Å from the methylenic hydrogen, H(7), or 0.4 Å less than the typical van der Waals H-H separation; as a consequence of this crowding, the B-H-B bridge is unsymmetrical and skewed toward B(10).

The  $\text{C}_4\text{B}_7$  cage geometry in III (and II) can usefully be described in several ways. The molecule may be viewed as a 13-vertex closo polyhedron<sup>14</sup> from which two nonadjacent vertices have been removed (Figure 7), which precisely fits the definition of an

arachno cage as a *closو* system with two missing vertices.<sup>17</sup> Compounds II and III are the first known carboranes with this geometry, although arachno- $[(C_6H_5)_3P]_2MC_2B_8H_{11}$  (M = Cu, Ag, Au) complexes are known.<sup>16</sup> Since II and III contain 28 skeletal electrons in an 11-vertex framework (based on contributions of three from each  $C-CH_3$  unit, two from each  $BH$ , and one from each "extra" hydrogen), they are  $(2n + 6)$ -electron systems in conformity<sup>5</sup> with the observed arachno geometry. If one compares II with the 11-vertex *closو* system  $C_2B_9H_{11}$ , a 24-electron  $(2n + 2)$  cage, the introduction of four skeletal electrons (as in II) is seen to produce cage-opening via lengthening of the four interactions between the apex atom [C(7)] and vertices 2, 3, 9, and 10.

Alternatively, one may regard the  $-CH(CH_3)-$  bridge as "outside" the cage and linked via two localized electron-pair bonds to the remaining  $(CH_3)_3C_3B_7H_8$  moiety, which is itself isoelectronic and isostructural with  $B_{10}H_{14}$ . In this sense, II and III would qualify as the first three-carbon analogues of  $B_{10}H_{14}$ .

NMR Spectra of II and III. As noted above, the  $^{11}B$  and  $^1H$  FT NMR spectra of the two species are closely similar, and they are entirely consistent with the crystallographically determined structure. The resonance at  $\delta \sim 7.3$  in III is assigned to B(11)-Br since no coupling to a terminal proton is observed; there is no indication in either spectrum of the presence of more than one isomer.

The  $^1H$  spectra (Figure 4) exhibit four nonequivalent methyl resonances, one of which is split into a doublet; this clearly arises from coupling of the methyl protons on C(M7) to the proton H(7). From the fact that C(2) and C(3) occupy similar coordination sites,

the closely spaced low-field methyl peaks can be cautiously assigned to the protons on C(M2) and C(M3), with the remaining resonance arising from the methyl group on C(M8).

The signal associated with the unique C-H proton H(7) proved elusive. Although its presence is clearly demonstrated by the splitting of the geminal methyl proton peak as noted, the C-H peak itself is not observable under normal conditions owing to its broad linewidth arising from unresolved coupling to (1) the adjacent methyl protons (giving a quartet with  $J = 6$  Hz), (2) the  $^{11}\text{B}$ (11) nucleus (doublet,  $J = 10$  to 30 Hz), and (3) the proton H(11) (doublet,  $J = 1$  to 10 Hz). However, with the aid of a triple resonance experiment<sup>18</sup> (broadband  $^{11}\text{B}$  decoupling plus single-frequency homonuclear decoupling), the collapse of the C(M7) doublet was observed by systematically positioning the homonuclear decoupler at frequencies in the expected range of H(7) ( $\delta$  3 to 1.5). When the desired collapse was achieved, the H(7) resonance was observed (Table II), coincident with a methyl resonance in both  $\text{C}_6\text{D}_6$  and  $\text{CDCl}_3$  solution. A similar experiment without  $^{11}\text{B}$  irradiation in  $\text{CDCl}_3$  produced collapse of the methyl doublet only under comparatively high power (6 mG) decoupling, which is consistent with the expectation that H(7) should resonate over a wide range in the absence of  $^{11}\text{B}$  decoupling. The observation of the H(7) peak at  $\delta$  2.3 in III (and the corresponding resonance at  $\delta$  2.45 in V, an isomer of II discussed below) reinforces these conclusions.

The chemical shift of H(7) may be compared with similar protons residing on bridging "methylenic" carbon atoms in other species; thus,

in  $R_2C_2B_{10}H_{11}^-$  ( $R = C_6H_5$  or  $CH_3$ ) (Figure 8, A) the shifts are  $\delta$  4.77 and 3.55, respectively.<sup>19</sup> In the former species, some deshielding undoubtedly occurs from the geminal phenyl group. In another carborane of this type,<sup>20</sup>  $(n^5-C_5H_5)Co(C_5H_4)^+-(CH_3)_4C_4B_8H_8^-$  (Figure 8, B) the bridging CH proton was not observed (though it was crystallographically located<sup>7</sup>), nor was the proton resonance arising from the geminal methyl group split into a doublet; this suggests tautomerization of the proton and/or fluxionality at rates faster than the reciprocal of the coupling constant.

Deprotonation of II and Conversion to a New Isomer. The treatment of  $(CH_3)_4C_4B_7H_9$  (II) with excess sodium hydride in THF produced one mole equivalent of  $H_2$  and generated a  $(CH_3)_4C_4B_7H_8^-$  monoanion (IV) as expected. However, re-protonation of this anion with HCl surprisingly failed to regenerate II, giving instead a different isomer (V) which was isolated in 27% yield as a white air-stable solid, m.p. 140°C.

The FT NMR spectra of IV and V indicate that both species have substantially different cage structures from II and III, and moreover that IV and V differ from each other. It is evident that deprotonation of II occurs at the bridging CH, and not the B-H-B bridge, since in the  $^1H$  NMR spectrum of IV, all four  $CH_3$  resonances are singlets and the B-H-B signal is still present. This result is not unexpected, since deprotonation of  $(CH_3)_2C_2B_7H_{11}$  also involves methylenic rather than BHB bridging protons.<sup>11c,21</sup> Also, Williams<sup>22</sup> has suggested a decreasing order of acidity as NH, SH > endo CH > BHB for arachno carboranes.

Removal of the CH proton in IV leaves the bridging carbon coordinately unsaturated, an unstable arrangement which probably induces movement of the bridging  $\text{CH}_3\text{C:}$  unit toward the B-H-B proton as shown in Figure 9. It would then seem reasonable for the bridging hydrogen to move to a new location between B(10) and B(11) as shown, thereby allowing C(7) to bond to B(9) and B(10) and hence achieve incorporation into the cage, as depicted in the suggested stable structure for the anion (IV). The geometry shown for IV is consistent with the  $^1\text{H}$  and  $^{11}\text{B}$  FT NMR and ir data, and represents a significantly altered cage geometry in comparison to the original species, II.

The re-protonation of IV could conceivably follow any of four paths: (1) regeneration of II, (2) reversal of the  $\text{CH}_3$  and H positions on C(7) relative to II, (3) protonation of the B(9)-B(10) edge in IV to form a second B-H-B bridge, causing C(7) to move into the framework between C(8) and B(9), or (4) entry of the proton at C(7) to form a  $-\text{CH}(\text{CH}_3)-$  bridge between C(8) and B(9), as shown in Figure 9(V). Possibility (1) is eliminated since II is not observed as a product, and (2) is effectively ruled out by the gross differences in the  $^{11}\text{B}$  NMR spectra of II and V; mere interchange of the  $\text{CH}_3$  and H ligands on C(7) in II would not produce major changes in the boron spectrum. Pathway (3) is eliminated by the appearance of a CH signal at  $\delta 2.45$ , the observation of an area 1 B-H-B resonance in V, and the fact that one of the methyl signals in the  $^1\text{H}$  spectrum is split into a doublet, indicating the presence of a  $-\text{CH}(\text{CH}_3)-$  bridge. The fourth possibility, however, is supported by the data and is depicted as

structure V in Figure 9. We emphasize that the geometries given for IV and V are not established, but represent likely arrangements consistent with available evidence.

### Conclusions

The degradation of  $(\text{CH}_3)_4\text{C}_4\text{B}_8\text{H}_8$  (I) to  $(\text{CH}_3)_4\text{C}_4\text{B}_7\text{H}_9$  (II) is illustrated in Figure 10. From comparison of the established structures of I and II, we envision that the boron removed is B(12), with C(7) accepting a proton and moving into the bridging position as shown; the second proton enters the B(9)-B(10) edge to form a B-H-B bridge. The base attack at B(12) indicates that this atom and its counterpart B(1) are the most electrophilic sites in I, consistent with their locations adjacent to two framework carbon atoms. This observation corroborates earlier indications<sup>23</sup> that the attack of  $\text{C}_2\text{H}_5\text{O}^-$  on I to form  $\text{B},\text{B}'-(\text{C}_2\text{H}_5\text{O})_2-(\text{CH}_3)_4\text{C}_4\text{B}_8\text{H}_6$  occurs at B(1) and B(12);<sup>24</sup> it also follows the pattern set by 1,2- $\text{C}_2\text{B}_{10}\text{H}_{12}$ , where the favored sites for base attack are B(3) and B(6),<sup>11a,b</sup> the borons adjacent to two carbon atoms.

The preference for a carbon-bridged structure in II, with placement of a proton on C(7) and movement of that atom out of the cage, is reasonable in that it permits C(7) to achieve a "normal" tetrahedral environment and also allows the remaining framework carbon atoms to adopt low-coordinate vertices on the open face. A similar argument was previously applied<sup>7</sup> to the  $(\text{CH}_3)_4\text{C}_4\text{B}_8\text{H}_9^-$  ion (Fig. 8B).

The fact that only one isomer of II is formed in the degradation implies a single stereospecific process. Similarly,

electrophilic bromination of II produces only one detectable isomer (though it is possible others may have formed in low yield), with attack occurring at B(11). This site is perhaps surprising, since in the  $C_2B_{10}H_{12}$  isomers electrophilic halogenation takes place preferentially at the boron atoms most distant from carbon.<sup>8</sup> Thus, in II one might have expected attack at B(5) or B(10); the fact that it occurs at B(11) indicates that the charge distribution in II is not controlled by simple inductive effects alone.

Finally, the formation of a new isomer of  $(CH_3)_4C_4B_7H_9$  (V) on deprotonation of II followed by treatment with HCl implies that V is thermodynamically favored over II (if it is assumed that facile kinetic pathways from the anion IV to both II and V are available). If the proposed structure for V is correct, the preference for V is understandable from the viewpoint that it is less strained than II and closer to icosahedral-fragment geometry. Further development of these ideas will depend on continuing chemical and structural investigations in this area.

Experimental Section

Materials. Tetra-C-methyltetracarbadodecacarborane(12),  $[(\text{CH}_3)_4\text{C}_4\text{B}_8\text{H}_8$ , (I)], was prepared from the complex  $[(\text{CH}_3)_2\text{C}_2\text{B}_4\text{H}_4]^2\text{FeH}_2$  as described elsewhere.<sup>2</sup> Tetrahydrofuran (THF) was dried over  $\text{LiAlH}_4$  prior to use.  $\text{NaH}$  (Alfa, 50% in mineral oil) was washed with pentane prior to use. Thin layer chromatography (TLC) was conducted on precoated plates of silica gel F-254 (Brinkmann Instruments, Inc.). All solvents were reagent grade.

Instrumentation.  $^{11}\text{B}$  (32 MHz) and  $^1\text{H}$  (100 MHz) pulse Fourier transform NMR spectra were recorded on a JEOL PS-100P spectrometer interfaced to a JEOL-Texas Instruments EC-100 computer system. Broadband heteronuclear decoupling was employed. 90-MHz  $^1\text{H}$  NMR spectra and some single-frequency homonuclear decoupling experiments were performed on a Varian EM-390 NMR spectrometer. Unit-resolution mass spectra (EI) were obtained on a Hitachi Perkin-Elmer RMU-6E mass spectrometer. Highresolution (CI) mass measurements were conducted on an ABI MS-902 double-focusing instrument equipped with an S<sub>ki</sub> chemical ionization source. Infrared spectra were recorded on a Beckman IR-8 instrument.

Synthesis of  $(\text{CH}_3)_4\text{C}_4\text{B}_7\text{H}_9$  (II) from  $(\text{CH}_3)_4\text{C}_4\text{B}_8\text{H}_8$  (I). In a typical reaction, 219 mg of I (1.07 mmol) was dissolved slowly in 25 ml 95% ethanol and

stirred in air. The progress of the reaction was monitored by spot TLC analysis in hexane (compound I  $R_f$  = 0.45) until no I was observed (about 12 hours.) The ethanol was removed by rotovap, with some warming of the flask. The residue was extracted with hexane, the solution filtered through 1 cm silica gel and the eluent was rotary-evaporated nearly to dryness. Residual solvent was removed by blowing dry  $N_2$  over the white solid to give 98.8 mg  $(CH_3)_4C_4B_7H_9$  (II, 0.51 mmol, 48% yield,  $R_f$  = 0.55 in hexane). The yield of II varied from 40-60%. The remaining residue in the flask was primarily  $B(OH)_3$  (45 mg, 68% yield), identified by ir and melting point. Similar reactions using lower and higher concentrations of  $H_2O$  in ethanol gave lower yields.

The following experiments represent attempts at increasing the yield of the reaction and determining the role of  $H_2O$  and solvent in the reaction.

$(CH_3)_4C_4B_8H_8$  in absolute ethanol: 89 mg of I was dissolved in 15 ml absolute ethanol (dried over molecular sieves) and stirred in vacuo for 8 hours. Spot TLC analysis showed only I. Subsequent work-up gave 87 mg of I (98% recovery).

$(CH_3)_4C_4B_8H_8$  in methanol: 10 mg of I was dissolved in about 10 ml methanol (dried over molecular sieves) and stirred in vacuo for 4 hours. Spot TLC analysis showed only I. The reaction vessel was then opened to the air and stirred for 12 hours, allowing the methanol to absorb water from the air and slowly evaporate. The residue in the

flask was purified by TLC to give 4 mg of II (40% yield).

$(CH_3)_4C_4B_8H_8$  in triethylamine: 10 mg of I was dissolved in 10 ml  $(C_2H_5)_3N$  (dried over BaO and  $P_2O_5$ ) and stirred in vacuo for 4 hours. Spot TLC analysis indicated only a trace of I. The  $(C_2H_5)_3N$  was removed by rotovap and the residue was purified by TLC to give about 1 mg of I.

$(CH_3)_4C_4B_8H_8$  in 5%  $H_2O$  in THF: 10 mg of I was dissolved in about 10 ml of 5%  $H_2O$  in THF and stirred in the air. Spot TLC analysis indicated only I after 15 minutes. After 6 hours, spot TLC showed neither I nor II.

$(CH_3)_4C_4B_7H_9$  in 95% ethanol: 30.1 mg of I was dissolved slowly in 15 ml 95% ethanol and stirred for 8 hours in air. The ethanol was removed at 30-35 °C using a rotary evaporator and the white residue was purified by TLC to give 22.8 mg II (75% recovery).

Direct Synthesis of II from  $(CH_3)_2C_2B_4H_5^-$  Ion.<sup>12</sup> A THF solution of  $Na^+[(CH_3)_2C_2B_4H_5]^-$ , prepared from 5.12 mmol of  $(CH_3)_2C_2B_4H_6$  and 5.85 mmol of NaH, was filtered under vacuum onto anhydrous  $FeCl_2$  at -196 °C. This mixture was allowed to come to room temperature, in contrast to previous preparations<sup>2</sup> of  $[(CH_3)_2C_2B_4H_4]FeH_2$  in which the temperature was held below -30 °C. After 1 hr the THF was removed under vacuum and  $CH_2Cl_2$  was added. The solution was stirred in air for 1 hr and the products were separated and purified via column and thin layer chromatography. In addition to previously reported compounds,<sup>2</sup> II was isolated in low yield. Mass measurement: calcd for  $^{12}C_8^{11}B_7^{1}H_{20}^+ (M + 1)$ , 193.2217, found 193.2223. The ir and FT NMR spectra were identical with those in Tables I-III.

Bromination of  $(CH_3)_4C_4B_7H_9$ . Under a nitrogen atmosphere, a 25 ml three-neck round bottom flask was charged with 41.6 mg  $AlCl_3$  (0.313 mmol, 1.3 equivalents, freshly sublimed in vacuo) and a magnetic stirbar. One port was affixed with an  $N_2$  inlet to maintain an overpressure of  $N_2$  and a second port was affixed with a tip-in sidearm containing 46.0 mg of II (0.239 mmol, 1.0 equivalents) dissolved in 5 ml of  $CS_2$  (dried over  $CaCl_2$  and over  $P_2O_5$ ). A 10.0 ml aliquot (0.29 mmol  $Br_2$ ) of a solution of 116.5 mg  $Br_2$  in 25.0 ml  $CS_2$  was put in a pressure-equalizing dropping funnel under a  $N_2$  flow at the third port. The  $Br_2$  solution was

added to the  $\text{AlCl}_3$ , with no apparent reaction, and the carborane was tipped into the reaction vessel. After 1 hour of stirring at room temperature with no apparent reaction the funnel was replaced by a reflux condenser and the solution was slowly refluxed for 5 hours, under  $\text{N}_2$ , giving a brownish-red solution and some light and dark precipitates. The reactor was then exposed to the air, the  $\text{CS}_2$  removed using a rotary evaporator, and the residue was dissolved in  $\text{CH}_2\text{Cl}_2$  and filtered through 1 cm silica gel and a glass frit. The  $\text{CH}_2\text{Cl}_2$  solution was rotovapped to give a cream-colored residue. TLC in 30%  $\text{CH}_2\text{Cl}_2$ /hexane ( $R_f = 0.6$ ) gave 32.5 mg of 11-Br- $(\text{CH}_3)_4\text{C}_4\text{B}_7\text{H}_8$  (III, 0.119 mmol, 50% yield).

Deprotonation of II. Synthesis of  $(\text{CH}_3)_4\text{C}_4\text{B}_7\text{H}_9$  (V). A 37-mg sample of II (0.19 mmol), 23 mg  $\text{NaH}$  (1.0 mmol), and a stirbar were placed in a tip-in sidearm flask which was evacuated and 15 ml dry THF was added by distillation in vacuo. The flask was slowly warmed to  $23^\circ\text{C}$ , vigorous bubbling ( $\text{H}_2$  evolution) occurring below  $0^\circ\text{C}$ . After stirring for 30 min ( $\text{H}_2$  evolution ceased) the solution was frozen,  $\text{H}_2$  pumped away (not measured, <sup>but</sup> see below) and after warming to  $23^\circ\text{C}$  the solution was filtered in vacuo into a lower flask containing a stirbar. (The sidearm flask containing residual  $\text{NaH}$  was removed under an  $\text{N}_2$  atmosphere and the port was plugged with a stopper.) The solution was frozen and 2.8 mmol  $\text{HCl}$  was transferred as a gas onto the frozen solution. The solution was then warmed to  $23^\circ\text{C}$  and stirred for 3 hr. The system was covered with  $\text{N}_2$ , exposed to the air, and the THF

removed by rotary evaporator. The white residue was purified by TLC in hexanes to give  $(\text{CH}_3)_4\text{C}_4\text{B}_7\text{H}_9$  (V, 10 mg, 27% yield,  $R_f = 0.45$ ) and a trace of an unidentified white compound at  $R_f = 0.60$ . The mass spectrum of V is closely similar to that of II, except that significant intensity is observed in the parent peaks at m/e 193 and 194, indicating that loss of 2H from V is less facile than from II (vide supra).

In a similar experiment, 60 mg II (0.31 mmol) was deprotonated with 37 mg NaH (1.5 mmol).  $\text{H}_2$  evolved was measured to be 0.33 mmol (106% of theory). The salt was filtered into an empty flask and the THF was removed in vacuo. In a dry box under an atmosphere of  $\text{N}_2$  the salt was dissolved in  $\text{CD}_3\text{CN}$  and filtered into an NMR tube (capped and wrapped with parafilm) for NMR analysis. Subsequent exposure to air indicated slow decomposition of the salt to an insoluble (in  $\text{CD}_3\text{CN}$ ) white solid. Before decomposition was complete, the  $\text{CD}_3\text{CN}$  was removed by a stream of  $\text{N}_2$  and the white residue was dissolved in 5 ml 95% ethanol and 1 ml 0.3M aqueous HCl. After stirring in air for 1 hr, the EtOH/ $\text{H}_2\text{O}$  was removed by rotary evaporator. TLC analysis showed only a trace of unidentified material at  $R_f = 0.35$  in hexane.

X-ray Structure Determination on

11-br- $(\text{CH}_3)_4\text{C}_4\text{B}_7\text{H}_8$ , (III). Single crystals of III

were grown by slow evaporation from  $\text{CDCl}_3$  at 10°C. One crystal was mounted on a glass fiber in an arbitrary orientation and examined by preliminary precession photographs which indicated acceptable crystal quality. Crystal data follow: Br $\text{C}_8\text{B}_7\text{H}_{20}$ ; molecular weight 271.84; space group

$P\bar{1}$ ,  $Z = 2$ ;  $a = 7.764(3)$ ,  $b = 8.352(5)$ ,  $c = 12.317(6) \text{ \AA}$ ,  $\alpha = 94.53(5)$ ,  $\beta = 95.41(5)$ ,  $\gamma = 120.51(5)^\circ$ ,  $V = 678 \text{ \AA}^3$ ,  $(\text{MoK}\alpha) = 31.8 \text{ cm}^{-1}$ ,  $\rho(\text{calcd}) = 1.34 \text{ g cm}^{-3}$ . Crystal dimensions (mm from centroid): -  $(100) 0.35$ ,  $(010) 0.23$ ,  $(0\bar{1}0) 0.23$ ,  $(1\bar{1}0) 0.24$ ,  $(\bar{1}10) 0.24$ ,  $(001) 0.055$ ,  $(00\bar{1}) 0.055$ .

For this crystal the Enraf-Nonius program SEARCH was used to obtain 25 accurately centered reflections which were then used in the program INDEX to obtain an orientation matrix for data collection and to provide approximate cell dimensions. Refined cell dimensions and their estimated standard deviations were obtained from 28 accurately centered reflections. The mosaicity of the crystal was examined by the  $\omega$  scan technique and judged to be satisfactory. The space group was chosen based on systematic absences and chemical and spectroscopic information. Successful solution and refinement of the structure confirmed the choice of space group.

Collection and Reduction of the Data. Diffraction data were collected at  $295^\circ\text{K}$  on an Enraf-Nonius four-circle CAD-4 diffractometer controlled by a PDP8/M computer using  $\text{MoK}\alpha$  radiation from a highly oriented graphite crystal monochromator. The  $\theta-2\theta$  scan technique was used to record the intensities of all reflections for which  $1.4^\circ < 2\theta < 48^\circ$ . Scan widths were calculated from the formula  $S_w = (A + B \tan \theta)$ , where  $A$  is estimated from the mosaicity of the crystal and  $B$  compensates for the increase in the width of the peak due to  $K_{\alpha_1}-K_{\alpha_2}$  splitting. The values of  $A$  and  $B$  were 0.60 and

0.35, respectively. The calculated scan angle was extended at each side by 25% for background determination (BG1 and BG2). The net count (NC) was then calculated as  $NC = TOT - 2(BG1 + BG2)$ , where TOT is the estimated peak intensity.

The intensities of four standard reflections, at 100 reflection intervals, showed no greater fluctuations during the data collection than those expected from Poisson statistics. The raw intensity data were corrected for Lorentz-polarization effects and then for absorption, (minimum transmission factor 0.46, maximum 0.78), resulting in 2038 reflections of which 1404 had  $F_o^2 > 3\sigma(F_o^2)$ , where  $(F_o^2)$  was estimated from counting statistics ( $\rho = 0.03$ ).<sup>26</sup> Only these latter data were used in the final refinement of the structural parameters.

Solution and Refinement of the Structure. Full-matrix least squares refinement was based on  $F$ , and the function minimized was  $w(|F_o| - |F_c|)^2$ . The weights  $w$  were taken as  $[2F_o/\sigma(F_o^2)]^2$ , where  $|F_o|$  and  $|F_c|$  are the observed and calculated structure factor amplitudes. The atomic scattering factors for nonhydrogen atoms were taken from Cromer and Waber<sup>27</sup> and those for hydrogen from Stewart, et al.<sup>28</sup> The effects of anomalous dispersion for all non-hydrogen atoms were included in  $F$  using the values of Cromer and Ibers<sup>29</sup> for  $\Delta f'$  and  $\Delta f''$ .

The position of the Br atom was determined from a three-dimensional Patterson function calculated from all the

intensity data. The intensity data were phased sufficiently well by these positional coordinates that difference Fourier syntheses revealed most of the non-hydrogen atoms, the remaining non-hydrogen atoms being inserted in calculated positions. Most of the cage hydrogen atoms were found from a Fourier difference map after introducing anisotropic thermal parameters for all non-hydrogen atoms. At least one hydrogen on each methyl group was found; the remaining hydrogen positions were calculated and inserted. The hydrogen atoms were included in the refinement for three cycles and thereafter held fixed. A final Fourier difference map was featureless. The error in an observation of unit weight was 1.96, and the largest parameter shift in the last cycle of refinement was 0.25 times the estimated standard deviation.

The model converged with  $R = 0.057$  and  $R_w = 0.063$ , where  $R = \sum ||F_o| - |F_c|| / \sum |F_o|$  and  $R_w = (\sum_w (|F_o| - |F_c|)^2 / \sum_w |F_o|^2)^{1/2}$ . Tables of observed and calculated structure factors are available (see paragraph at end of paper on supplementary material.) The computing system and programs are described elsewhere.<sup>30</sup>

Acknowledgments. This work was supported by the Office of Naval Research and the National Science Foundation, Grant CHE 79-09948. We are grateful to Mr. William Hutton for assistance in recording the NMR spectra and to Professor Ekk Sinn for assistance in the X-ray structure determination.

Supplementary Material Available: Listing of observed and calculated structure factors ( 6 pages). Ordering information is given on any current masthead page.

References and Notes

- (1) Based in part on a Ph.D. dissertation (University of Virginia, 1980) by D.C.F.
- (2) Maxwell, W.M.; Miller, V.R.; Grimes, R.N. Inorg. Chem. 1976, 15, 1343.
- (3) Grimes, R.N.; Sinn, E.; Pipal, J.R. Inorg. Chem. 1980, 19, 2087, and references therein.
- (4) This term is used in a relative descriptive sense, to indicate the presence of excess skeletal electrons beyond the  $2n + 2$  normally required to fill the  $n + 1$  bonding molecular orbitals in a closo  $n$ -vertex polyhedron.<sup>5</sup>
- (5) (a) Wade, K. Adv. Inorg. Chem. Radiochem. 1976, 18, 1; (b) Mingos, D.M.P. Nature (London), Phys. Sci. 1972, 236, 99; (c) Rudolph, R.W. Acc. Chem. Res. 1976, 9, 446.
- (6) Grimes, R.N. Acc. Chem. Res. 1978, 11, 420.
- (7) Grimes, R.N.; Pipal, J.R.; Sinn, E. J. Am. Chem. Soc. 1979, 101, 4172.
- (8) Beall, H. in "Boron Hydride Chemistry"; Muetterties, E.L., Ed.; Academic Press: New York, 1975.
- (9) Freyberg, D.P.; Weiss, R.; Sinn, E.; Grimes, R.N. Inorg. Chem. 1977, 16, 1847.
- (10) Grimes, R.N.; Maxwell, W.M.; Maynard, R.B.; Sinn, E. Inorg. Chem. 1980, 19, 0000.
- (11) (a) Wiesboeck, R.A.; Hawthorne, M.F. J. Am. Chem. Soc. 1964, 86, 1642; (b) Zakharkin, L.I.; Kalinin, V.N. Dokl. Akad. Nauk SSSR 1965, 163, 110. (c) Tebbe, F.N.; Garrett, P.M.; Hawthorne, M.F. J. Am. Chem. Soc. 1968, 90, 869.

(12) Weiss, R.; Grimes, R.N., unpublished results.

(13) Pipal, J.R.; Grimes, R.N. Inorg. Chem. 1978, 17, 10.

(14) Closo metallacarboranes of 13 vertices have been structurally characterized,<sup>15a</sup> and the same geometry (corresponding to that shown in Fig. 7) has been calculated<sup>15b,c</sup> for  $B_{13}H_{13}^{2-}$ .

(15)(a) Churchill, M.R.; DeBoer, B.G. Inorg. Chem. 1974, 13, 1411;  
(b) Brown, L.D.; Lipscomb, W.N. Inorg. Chem. 1977, 16, 2989;  
(c) Bicerano, J.; Marynick, D.S.; Lipscomb, W.N. ibid. 1978, 17, 3443;

(16) Colquhoun, H.M.; Greenhough, T.J.; Wallbridge, M.G.H. J. Chem. Soc., Chem. Commun., 1980, 192.

(17) Williams, R.E. Inorg. Chem. 1971, 10, 210.

(18) Miller, V.R.; Grimes, R.N. Inorg. Chem. 1977, 16, 15.

(19)(a) Dunks, G.B.; Wiersema, R.J.; Hawthorne, M.F. J. Am. Chem. Soc. 1973, 95, 3174; (b) Tolpin, E.I.; Lipscomb, W.N. Inorg. Chem. 1973, 12, 2257.

(20) Maxwell, W.M.; Grimes, R.N. Inorg. Chem. 1979, 18, 2174.

(21) Voet, D.; Lipscomb, W.N. Inorg. Chem. 1967, 6, 113.

(22) Williams, R.E. Adv. Inorg. Chem. Radiochem. 1976, 18, 67.

(23) Maxwell, W.M.; Wong, K-S.; Grimes, R.N. Inorg. Chem. 1977, 16, 3094.

(24) NMR data<sup>23</sup> show that the diethoxy species is symmetrically substituted, but there are four pairs of equivalent boron vertices on  $(CH_3)_4C_4B_8H_8$  at which such substitution could occur. However, the fact that the ethoxy group on an analogous cobaltacarborane,  $(\eta^5-C_5H_5)Co(CH_3)_4C_4B_7H_7$  (isomer I), is located at B(12)<sup>25</sup> is taken as support for 1,12 di-substitution on  $(CH_3)_4C_4B_8H_8$  itself.

- (25) Pipal, J.R.; Grimes, R.N. J. Am. Chem. Soc. 1978, 100, 3083.
- (26) Corfield, P.W.R.; Doedens, R.J.; Ibers, J.A., Inorg. Chem., 1967, 6, 197.
- (27) Cromer, D.T.; Waber, J.T., "International Tables for X-ray Crystallography," Vol. IV, the Kynoch Press, Birmingham, England, 1974.
- (28) Stewart, R.F.; Davidson, E.R.; Simpson, W.T.; J. Chem. Phys., 1965, 42, 3175.
- (29) Cromer, D.T.; Ibers, J.A., ref. 27.
- (30) Freyberg, D.P.; Mockler, G.M.; Sinn, E., J. Chem. Soc., Dalton Trans. 1976, 447.

Table I. 32.1 MHz  $^{11}\text{B}$  FT NMR Data.<sup>a</sup>

Compound	Chemical Shift, ppm <sup>b</sup> (J, Hz.)	Rel area
II, $(\text{CH}_3)_4\text{C}_4\text{B}_7\text{H}_9$	8.7 (126) 2.9 (181) -3.3 (156) -7.3 (150) -11.1 (180) -41.7 (156)	1 2 1 1 1 1
III, $(\text{CH}_3)_4\text{C}_4\text{B}_7\text{H}_8\text{Br}$	8.4 (156) 0.5 (166) -2.2 (150) -7.3 -8.6 (182) -41.7 (156)	1 2 1 1 1 1
IV <sup>c</sup> , $\text{Na}^+ (\text{CH}_3)_4\text{C}_4\text{B}_7\text{H}_8^-$	7.6 (116) 2.7 (132) -4.3 (147) -17.1 (122) -26.8 (146)	1 1 2 1 2

(Continued)

$\nu, (\text{CH}_3)_4\text{C}_4\text{B}_7\text{H}_9$ , Second Isomer	4.4 (147)	3
	-7.8 d	1
	-10.5 d	1
	-12.0 d	1
	-40.3 (156)	1

<sup>a</sup> Spectra obtained in  $\text{CDCl}_3$ , except where otherwise noted.

<sup>b</sup>  $\text{BF}_3 \cdot \text{O}(\text{C}_2\text{H}_5)_2 = 0$ , positive shifts downfield.

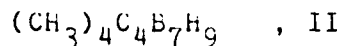
<sup>c</sup> Spectrum obtained in  $\text{CD}_3\text{CN}$ . <sup>d</sup>  $J_{\text{BH}}$  coupling obscured by peak overlap.

Table II. 100 MHz  $^1\text{H}$  NMR Data

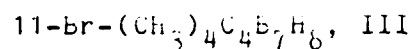
Compound (solvent)	Chemical shifts, $\delta$ , in ppm <sup>a</sup>				
	CH <sub>3</sub> (area 3)	CH <sub>3</sub> (7) <sup>b</sup> (area 3)	H (7) (area 1)	BH (area 1)	BH (area)
II (CDCl <sub>3</sub> )	2.02 1.95 1.30	1.08	2.04	-1.65 <sup>c</sup>	3.7(1) 2.9(1) 2.5(1) 2.4(2) 1.3(1) 0.4(1)
II (C <sub>6</sub> D <sub>6</sub> )	1.81 1.39 0.89	0.87	1.8	-1.57 <sup>c</sup>	3.8(1) 3.5(1) 3.0(3) 2.5(1) 1.6(1)
III (CDCl <sub>3</sub> )	2.01 1.95 1.33	1.09	2.3	-1.3 <sup>c</sup>	3.7(1) 3.6(1) 3.1(1) 2.9(1) 2.6(1) 1.6(1) 0.4(1)
IV (CD <sub>3</sub> CN)	1.98 1.55 1.05 0.99			-1.53 <sup>d</sup>	e
V (CDCl <sub>3</sub> )	1.97 1.90 1.15	1.22	2.45	f	e
V (C <sub>6</sub> D <sub>6</sub> )	1.73 1.29 0.71	0.97	2.2	-1.65 <sup>c</sup>	e

<sup>a</sup>Shifts referenced to (CH<sub>3</sub>)<sub>4</sub>Si. <sup>b</sup>Doublet due to coupling to CH(7),  $J_{\text{HH}} \approx 6$  Hz. <sup>c</sup>Doublet of doublets, apparent 1:2:1 triplet,  $J_{\text{HH}} = 10$  Hz. <sup>d</sup>Apparent 1:3:3:1 quartet(?),  $J_{\text{HH}} = 10$  Hz. <sup>e</sup>BH protons not readily distinguished. <sup>f</sup>Spectrum obtained without <sup>11</sup>B-decoupling; bridge hydrogens not observed.

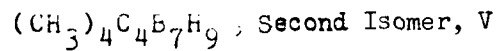
Table III. Ir Data, (cm<sup>-1</sup>, KBr pellet.)



2960s, 2930s, 2880s, 2600sh, 2560s, 2480s, 1950wbr,  
1620wbr, 1565wbr, 1440s, 1395m, 1385s, 1365s, 1340w,  
1250m, 1220w, 1150m, 1100m, 1080m, 1025s, 1005m, 980s,  
910s, 800s, 780s, 720, 700m, 680w.



2960s, 2920s, 2860s, 2570sbr, 1950wbr, 1725wbr,  
1560wbr, 1440s, 1395m, 1385s, 1365s, 1340m, 1260s,  
1230m, 1195m, 1155m, 1070sbr, 1020sbr, 1000sh, 990m,  
980m, 935m, 910m, 880sh, 855s, 795sbr, 725m, 700w,  
695w, 660w, 625m.



2960s, 2930s, 2870m, 2830m, 2590sbr, 2480s, 1975wbr,  
1530wbr, 1550wbr, 1460sh, 1450s, 1380s, 1320w, 1250w,  
1230w, 1160w, 1120w, 1070s, 1040w, 1005s, 985s, 910s,  
810s, 780w, 760w, 720s, 700m, 665w, 640w.

s = strong, m = medium, w = weak, br = broad, sh = shoulder.

TABLE IV. POSITIONAL AND THERMAL PARAMETERS AND THE IP ESTIMATED STANDARD DEVIATIONS FOR 11-Br-(CH<sub>3</sub>)<sub>4</sub>C<sub>6</sub>B7B<sub>8</sub> (III)<sup>a</sup>

ATOM	X	Y	Z	U11	U22	U33	U12	U13	U23
BP	0.3661(1)	0.23558(8)	0.09339(7)	0.1673(4)	0.0586(2)	0.0685(5)	0.0496(2)	-0.0162(4)	-0.0123(3)
C(2)	0.3532(6)	0.7555(7)	0.3153(5)	0.050(3)	0.048(2)	0.058(4)	0.024(2)	0.012(3)	0.007(2)
C(3)	0.3113(8)	0.5529(6)	0.2355(5)	0.054(3)	0.043(2)	0.052(3)	0.026(2)	0.005(3)	0.012(2)
C(7)	0.3131(2)	0.6729(7)	0.1214(5)	0.070(5)	0.041(2)	0.048(4)	0.043(2)	0.007(3)	0.007(2)
C(8)	0.3530(5)	0.5525(7)	0.2153(5)	0.053(3)	0.045(2)	0.053(4)	0.023(2)	0.017(3)	0.015(2)
C(12)	0.2571(4)	0.8768(9)	0.3601(6)	0.056(3)	0.075(3)	0.087(5)	0.026(2)	0.006(3)	0.004(3)
C(15)	0.4152(5)	0.4444(8)	0.3200(6)	0.085(3)	0.070(3)	0.072(4)	0.043(2)	-0.002(3)	0.010(3)
C(17)	0.4447(10)	0.6810(8)	0.0767(6)	0.094(3)	0.080(3)	0.063(4)	0.060(2)	0.017(3)	0.011(3)
C(19)	0.4942(10)	1.0335(8)	0.1510(6)	0.079(3)	0.055(3)	0.105(5)	0.029(3)	0.035(4)	0.032(3)
B(1)	0.263(1)	0.6583(9)	0.4055(7)	0.060(3)	0.051(3)	0.063(5)	0.027(2)	0.009(4)	0.005(3)
B(4)	0.065(1)	0.4601(8)	0.3084(7)	0.059(3)	0.045(3)	0.071(5)	0.023(2)	0.006(4)	0.014(3)
B(5)	0.345(1)	0.6634(9)	0.3513(7)	0.055(4)	0.061(3)	0.063(5)	0.035(2)	0.008(4)	0.008(3)
B(6)	0.294(1)	0.8577(3)	0.3381(6)	0.067(4)	0.052(3)	0.059(5)	0.030(2)	0.011(3)	0.005(3)
B(9)	0.1949(10)	0.7929(8)	0.2367(7)	0.057(3)	0.050(3)	0.073(5)	0.037(2)	0.012(3)	0.012(3)
B(10)	-0.353(1)	0.5386(9)	0.2176(7)	0.064(3)	0.059(3)	0.052(5)	0.020(2)	0.011(4)	0.018(3)
B(11)	0.153(1)	0.4889(8)	0.1787(6)	0.065(3)	0.045(3)	0.054(4)	0.033(2)	0.002(3)	0.003(3)
ATOM b	X	Y	Z	B <sub>1</sub>	B <sub>2</sub>	ATOM b	X	Y	Z
H(21)	0.771(6)	1.018(7)	0.385(5)	6.0(1)	H(8)	0.616(7)	1.643(6)	0.172(4)	4.7(1)
H(22)	0.671(7)	0.834(7)	0.423(5)	5.0(1)	H(62)	0.554(8)	1.145(7)	0.257(5)	5.0(1)
H(23)	0.725(3)	0.868(7)	0.305(5)	6.0(2)	H(63)	0.428(8)	1.062(7)	0.138(5)	6.0(1)
H(51)	0.312(8)	0.329(7)	0.334(5)	6.0(1)	H(4)	-0.014(7)	0.350(6)	0.336(4)	4.0(1)
H(32)	0.503(8)	0.501(7)	0.405(5)	7.0(2)	H(5)	-0.057(7)	0.688(7)	0.424(4)	4.0(1)
H(33)	0.463(9)	0.433(8)	0.266(5)	7.0(2)	H(6)	0.577(7)	0.995(6)	0.404(4)	4.0(1)
H(71)	0.542(7)	0.647(7)	0.126(5)	5.0(1)	H(7)	0.204(7)	0.678(6)	0.060(4)	4.0(1)
H(72)	0.553(8)	0.611(8)	0.051(5)	6.0(2)	H(9)	0.051(7)	0.895(6)	0.220(4)	4.0(1)
H(73)	0.465(6)	0.590(7)	0.019(4)	5.0(1)	H(90)	0.061(7)	0.657(6)	0.154(4)	4.0(1)
				H(10)	-0.195(6)	0.481(7)	0.193(5)	0.063(3)	0.063(3)

<sup>a</sup> The form of the unisotopic thermal parameter is  $\text{exp}[-2\pi^2(U_{11}h^2a^{*2} + U_{12}k^2b^{*2} + U_{13}l^2c^{*2} + 2U_{11}hka^*b^* + 2U_{12}hkb^*c^* + 2U_{13}hlc^*b^*]$ . Standard isotopic B values are given for hydrogen atoms.

Table V. Bond Lengths (Å) in 11-Br-(CH<sub>3</sub>)<sub>4</sub>C<sub>4</sub>B<sub>7</sub>H<sub>8</sub> (III)

B(1)-C(2)	1.692(6)	B(6)-B(11)	1.770(7)
B(1)-C(3)	1.735(6)	C(7)-C(8)	1.546(5)
B(1)-B(4)	1.773(6)	C(7)-C(11)	1.616(6)
B(1)-B(5)	1.804(7)	C(7)-C(M7)	1.517(5)
B(1)-B(6)	1.771(6)	C(7)-H(7)	0.952(3)
C(2)-C(3)	1.516(4)	C(8)-B(9)	1.846(6)
C(2)-B(6)	1.660(6)	C(8)-C(M8)	1.531(5)
C(2)-B(11)	1.698(5)	B(9)-B(10)	1.811(6)
C(2)-C(M2)	1.519(5)	B(9)-H(910)	1.301(4)
C(3)-B(4)	1.685(6)	B(10)-B(11)	1.937(6)
C(3)-C(8)	1.611(5)	B(10)-H(910)	1.236(6)
C(3)-C(M3)	1.512(5)	B(11)-Br	1.994(4)
B(4)-B(5)	1.771(7)	$\langle B-H_{\text{terminal}} \rangle$	1.097
B(4)-C(8)	1.752(6)	$\langle C-H_{\text{methyl}} \rangle$	0.957
B(4)-B(9)	1.758(7)	Nonbonded Distances	
B(5)-B(6)	1.806(6)	C(7)-C(2)	2.52
B(5)-B(9)	1.781(6)	C(7)-C(3)	2.43
B(5)-B(10)	1.768(7)	C(7)-B(9)	2.59
B(6)-B(10)	1.712(6)	C(7)-B(10)	2.70
		H(7)-H(910)	1.99

Table VI. Bond Angles (deg) in 11-Br-(CH<sub>3</sub>)<sub>4</sub>C<sub>4</sub>B<sub>7</sub>H<sub>8</sub> (II<sup>-</sup>)

C(2)-B(1)-C(3)	52.5(2)	B(1)-B(6)-B(11)	108.3(3)
C(3)-B(1)-B(4)	57.4(2)	C(2)-B(6)-B(5)	107.4(3)
B(4)-B(1)-B(5)	59.3(2)	C(2)-B(6)-B(10)	115.6(3)
B(5)-B(1)-B(6)	60.7(3)	C(2)-B(6)-B(11)	59.2(2)
B(6)-B(1)-B(2)	57.2(2)	B(5)-B(6)-B(10)	60.3(3)
B(1)-C(2)-B(3)	65.2(3)	B(5)-B(6)-B(11)	110.3(3)
B(1)-C(2)-B(6)	63.8(3)	B(10)-B(6)-B(11)	67.6(3)
B(1)-C(2)-B(11)	115.7(3)	C(8)-C(7)-B(11)	102.7(3)
B(1)-C(2)-C(M2)	116.8(3)	C(8)-C(7)-C(M7)	111.3(3)
C(3)-C(2)-B(6)	111.9(3)	C(8)-C(7)-H(7)	111.9(3)
C(3)-C(2)-B(11)	104.8(3)	B(11)-C(7)-C(M7)	113.5(3)
C(3)-C(2)-C(M2)	120.2(3)	B(11)-C(7)-H(7)	111.2(3)
B(6)-C(2)-B(11)	63.6(3)	C(M7)-C(7)-H(7)	106.3(3)
B(6)-C(2)-C(M2)	121.6(3)	C(3)-B(8)-C(4)	60.0(2)
B(11)-C(2)-C(M2)	121.0(3)	C(3)-C(8)-C(7)	100.8(3)
B(1)-C(3)-C(2)	62.3(2)	C(3)-C(8)-B(9)	108.3(3)
B(1)-C(3)-B(4)	62.4(2)	C(3)-C(8)-C(M8)	116.9(3)
B(1)-C(3)-B(8)	114.5(3)	B(4)-B(8)-C(7)	136.1(3)
B(1)-C(3)-C(M3)	118.6(3)	B(4)-B(8)-B(9)	58.4(2)
B(2)-C(3)-C(4)	111.6(3)	B(4)-C(8)-C(M8)	107.8(3)
C(2)-C(3)-B(8)	108.7(3)	C(7)-B(8)-B(9)	99.0(3)
C(2)-C(3)-C(M3)	121.6(3)	C(7)-C(8)-C(M8)	116.0(2)
B(4)-C(3)-C(8)	64.2(2)	B(9)-C(8)-C(M8)	113.7(2)
B(4)-C(3)-C(M3)	118.4(3)	B(4)-B(9)-B(5)	60.0(3)
C(8)-C(3)-C(M3)	118.7(3)	B(4)-B(9)-C(8)	58.1(2)
B(1)-B(4)-C(3)	60.1(2)	B(4)-B(9)-B(10)	105.9(3)

(continued)

B(1)-B(4)-B(5)	61.2(3)	B(5)-B(9)-C(8)	103.8(3)
B(1)-B(4)-C(8)	106.0(3)	B(5)-B(9)-B(10)	59.0(3)
B(1)-B(4)-B(9)	111.4(3)	C(8)-B(9)-B(10)	102.2(3)
C(3)-B(4)-B(5)	107.6(3)	B(10)-B(9)-H(910)	43.0(2)
C(3)-B(4)-C(8)	55.9(2)	B(5)-B(10)-B(6)	62.5(2)
C(3)-B(4)-B(9)	109.1(3)	B(5)-B(10)-B(9)	59.7(3)
B(5)-B(4)-C(8)	108.3(3)	B(5)-B(10)-B(11)	104.7(3)
B(5)-B(4)-B(9)	60.6(3)	B(6)-B(10)-B(9)	105.6(3)
C(8)-B(4)-B(9)	63.5(2)	B(6)-B(10)-B(11)	57.6(3)
B(1)-B(5)-B(4)	59.5(3)	B(9)-B(10)-B(11)	97.8(3)
B(1)-B(5)-B(6)	58.7(2)	B(9)-B(10)-H(910)	45.9(2)
B(1)-B(5)-B(9)	109.0(3)	C(2)-B(11)-B(6)	57.1(2)
B(1)-B(5)-B(10)	108.9(3)	C(2)-B(11)-C(7)	99.1(3)
B(4)-B(5)-B(6)	101.0(3)	C(2)-C(11)-B(10)	103.2(3)
B(4)-B(5)-B(9)	59.3(3)	C(2)-B(11)-Br	116.6(2)
B(4)-B(5)-B(10)	107.2(3)	B(6)-B(11)-C(7)	130.0(3)
B(6)-B(5)-B(9)	103.3(3)	B(6)-B(11)-B(10)	54.8(2)
B(6)-B(5)-B(10)	57.2(2)	B(6)-B(11)-Br	112.6(3)
B(9)-B(5)-B(10)	61.4(3)	C(7)-B(11)-B(10)	98.7(3)
B(1)-B(6)-C(2)	59.0(2)	C(7)-B(1)-Br	117.4(3)
B(1)-B(6)-B(5)	60.5(3)	B(10)-B(11)-Br	118.6(3)
B(1)-B(6)-B(10)	113.1(3)	B(9)-H(910)-B(10)	91.1(3)

Table VII. Selected Mean Planes in 11-Br-(CH<sub>3</sub>)<sub>4</sub>C<sub>4</sub>B<sub>7</sub>H<sub>8</sub>

atom	dev, $\text{\AA}$	atom	dev, $\text{\AA}$
Plane 1: C(2), C(3), B(4), B(5), B(6)			
$-0.1892x + 0.1625y - 0.9684z = -2.8690$			
C(2)	-0.0433	B(6)	0.0487
C(3)	0.0154	C(M2)	-0.7625
B(4)	0.0168	C(M3)	-0.6252
B(5)	-0.0376	B(1)	-1.0113
Plane 2: B(9), B(10), H(910)			
$0.9973x - 0.0369y - 0.0641z = -3.2367$			
B(9)	0.0000	H(910)	0.0000
B(10)	0.0000	B(5)	-0.0774
Plane 3: C(8), B(9), B(10), B(11)			
$-0.1951x + 0.1642y - 0.9669z = -1.3785$			
C(8)	-0.0209	C(7)	0.8680
B(9)	0.0283	H(910)	0.8776
B(10)	-0.0270	C(M8)	0.4519
B(11)	0.0196	Br	0.6518
Plane 4: C(2), C(3), B(8), B(11)			
$0.8563x + 0.0770y - 0.5106z = -1.8069$			
C(2)	-0.0204	C(M2)	0.7688
C(3)	0.0213	C(M3)	0.8424
C(8)	-0.0132	C(M8)	0.5182
B(11)	0.0123	C(7)	0.7342
		Br	0.8215
Plane 5: C(2), C(3), B(9), B(10)			
$0.3509x + 0.1063y - 0.9304z = -3.1173$			
C(2)	0.0026	C(M2)	0.0001
C(3)	-0.0026	C(M3)	-0.0044
B(9)	0.0022	H(910)	0.8110
B(10)	-0.0022		

atom	dev, $\text{\AA}^\circ$	atom	dev, $\text{\AA}^\circ$
Plane 6: C(7), C(8), B(11)			
$-0.9560x + 0.0611y - 0.2868z = 0.6159$			
C(7)	0.0000	Br	-0.2629
C(8)	0.0000	B(4)	0.2066
B(11)	0.0000	B(6)	0.2177
C(M8)	-0.1187	C(M7)	-1.2010
Plane 7: B(1), B(4), B(9), B(10), B(6)			
$0.7808x + 0.0812y = 0.6195z = -3.5933$			
B(1)	-0.0804	B(6)	0.0897
B(4)	0.0446	H(910)	0.4841
B(9)	0.0061	B(5)	-0.9712
B(10)	-0.0600		

Dihedral Angles Between Planes

planes	angle, deg	planes	angle, deg
1,2	97.62	3,4	70.16
1,3	0.36	3,5	31.94
1,4	69.82	3,6	61.71
1,5	31.59	3,7	62.61
1,6	62.06	4,5	38.40
1,7	62.27	4,6	131.88
2,3	97.97	4,7	7.60
2,4	27.89	5,6	93.56
2,5	66.07	5,7	30.80
2,6	159.60	6,7	124.32
2,7	35.38		

Figure Captions

Figure 1. Equilibrium<sup>7</sup> between  $(\text{CH}_3)_4\text{C}_4\text{B}_8\text{H}_8$  isomers A (established) and B (proposed). Solid circles represent C-CH<sub>3</sub> groups; other vertices are BH.

Figure 2. Mass spectroscopic parent group intensities for II [ $(\text{CH}_3)_4\text{C}_4\text{B}_7\text{H}_9$ ] and III [ $(\text{CH}_3)_4\text{C}_4\text{B}_7\text{H}_8\text{Br}$ ], with horizontal scales in units of m/e. II (a), calculated for  $(\text{CH}_3)_4\text{C}_4\text{B}_7\text{H}_7$ ; II (b), electron-impact (EI) spectrum of II; II (c), chemical ionization (CI) spectrum in CH<sub>4</sub>. III (a), calculated for  $(\text{CH}_3)_4\text{C}_4\text{B}_7\text{H}_8\text{Br}$ ; III (b), EI spectrum; III (c), CI spectrum in CH<sub>4</sub>. CI spectra exhibit cutoffs one mass unit higher than EI spectra due to protonation by methane. For both compounds, CI spectra in Ar/H<sub>2</sub>O are similar to the spectra in CH<sub>4</sub> except for the appearance of M + 17 peaks arising from hydration.

Figure 3. 32.1-MHz proton-decoupled <sup>11</sup>B FT NMR spectra of II, III, and V (CDCl<sub>3</sub> solution) and IV (CD<sub>3</sub>CN). Chemical shifts and coupling constants are given in Table I.

Figure 4. Simplified representations of the H-C <sup>1</sup>H FT NMR resonances of II, III, IV, and V. The H-C<sub>bridge</sub> signals are shown as small broad peaks, the methyl singlets as tall lines, and the methyl doublets as shorter lines.

Figure 5. Stereoview of the molecular structure of III [ $11\text{-Br-}(\text{CH}_3)_4\text{C}_4\text{B}_7\text{H}_8$ ], with nonhydrogen atoms shown as 50% thermal ellipsoids. Hydrogens other than H(7) and H(910) are omitted for clarity. H(7) and H(910) are depicted as spheres of arbitrary radius.

Figure 6. Unit cell packing of III.

Figure 7. (A) Cage geometry of III depicted as an arachno fragment of a 13-vertex closo polyhedron (B).

Figure 8. Established structures of other carborane species with bridging carbon atoms: A,  $\text{R}_2\text{C}_2\text{B}_{10}\text{H}_{11}^-$  ( $\text{R} = \text{CH}_3, \text{C}_6\text{H}_5$ ),<sup>11a,b</sup> B,  $(\text{CH}_3)_4\text{C}_4\text{B}_8\text{H}_9^-$  (characterized as a cobaltocene derivative).<sup>7</sup> Framework carbon atoms and BH units are depicted as solid and open circles, respectively.

Figure 9. Scheme for conversion of  $(\text{CH}_3)_4\text{C}_4\text{B}_7\text{H}_9$  (II) to  $(\text{CH}_3)_4\text{C}_4\text{B}_7\text{H}_8^-$  ion (IV) and  $(\text{CH}_3)_4\text{C}_4\text{B}_7\text{H}_9$  (V), showing proposed structures of IV, V, and a possible intermediate species. Solid circles indicate framework carbon locations; other vertices are BH.

Figure 10. Scheme for formation of  $(\text{CH}_3)_4\text{C}_4\text{B}_7\text{H}_9$  (II) by degradation of  $(\text{CH}_3)_4\text{C}_4\text{B}_8\text{H}_8$  (I, isomer B). Solid circles indicate framework carbon atoms.

Fig. 1.

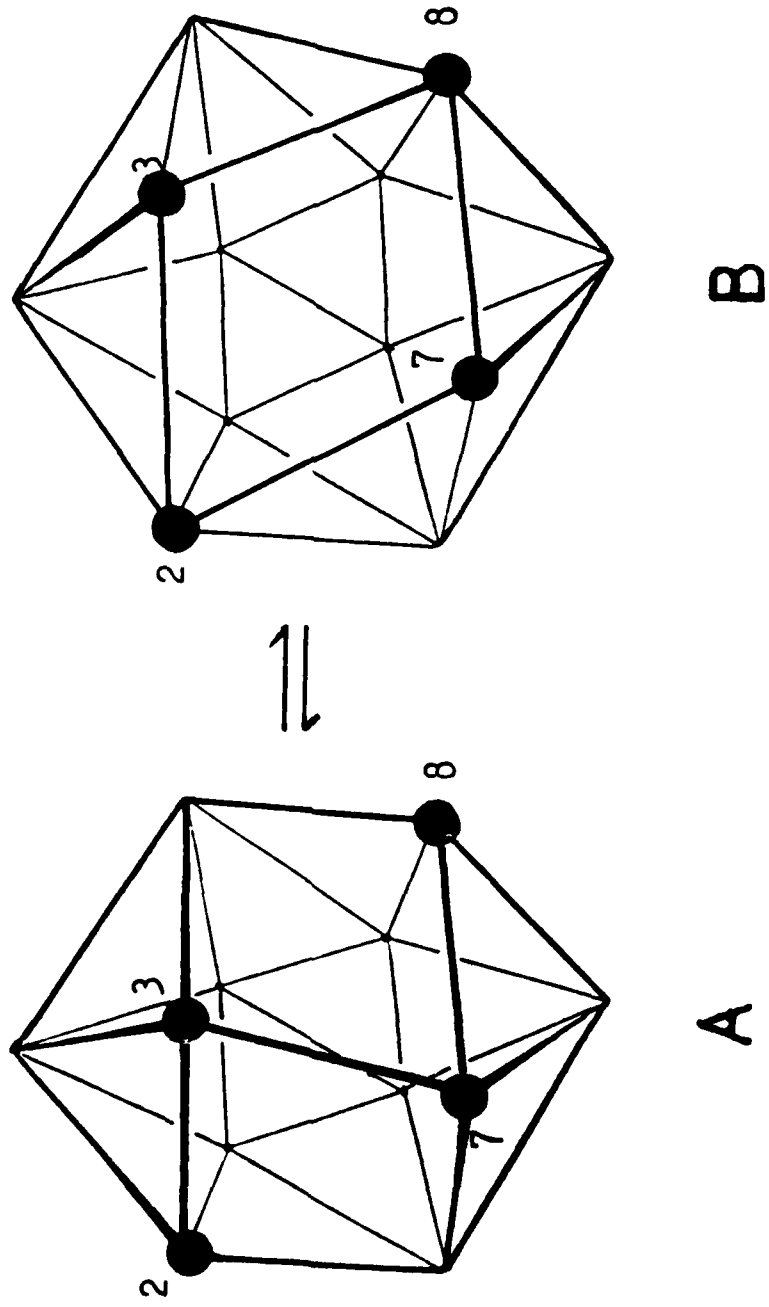


Fig. 2

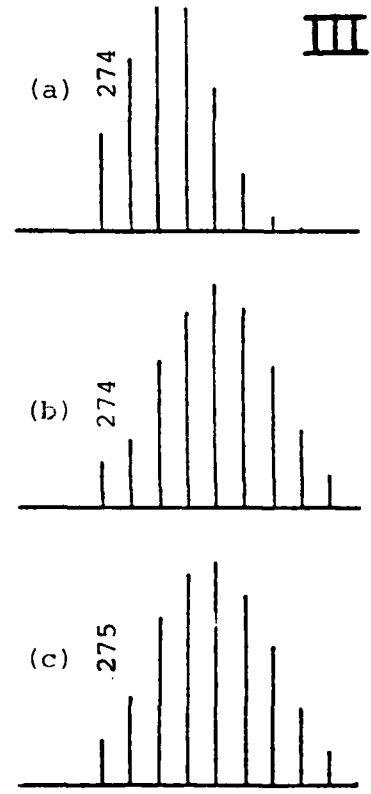
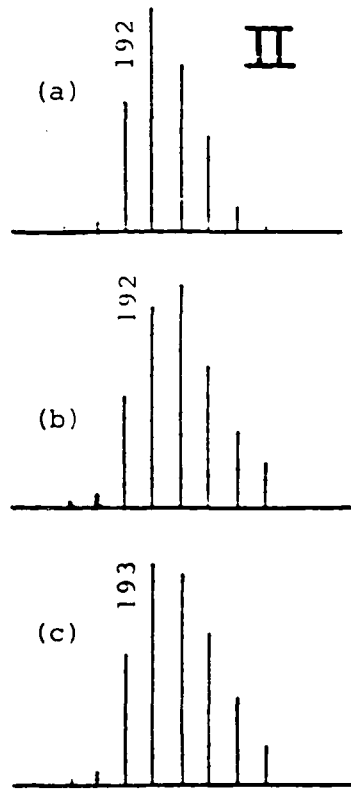


Fig. 3

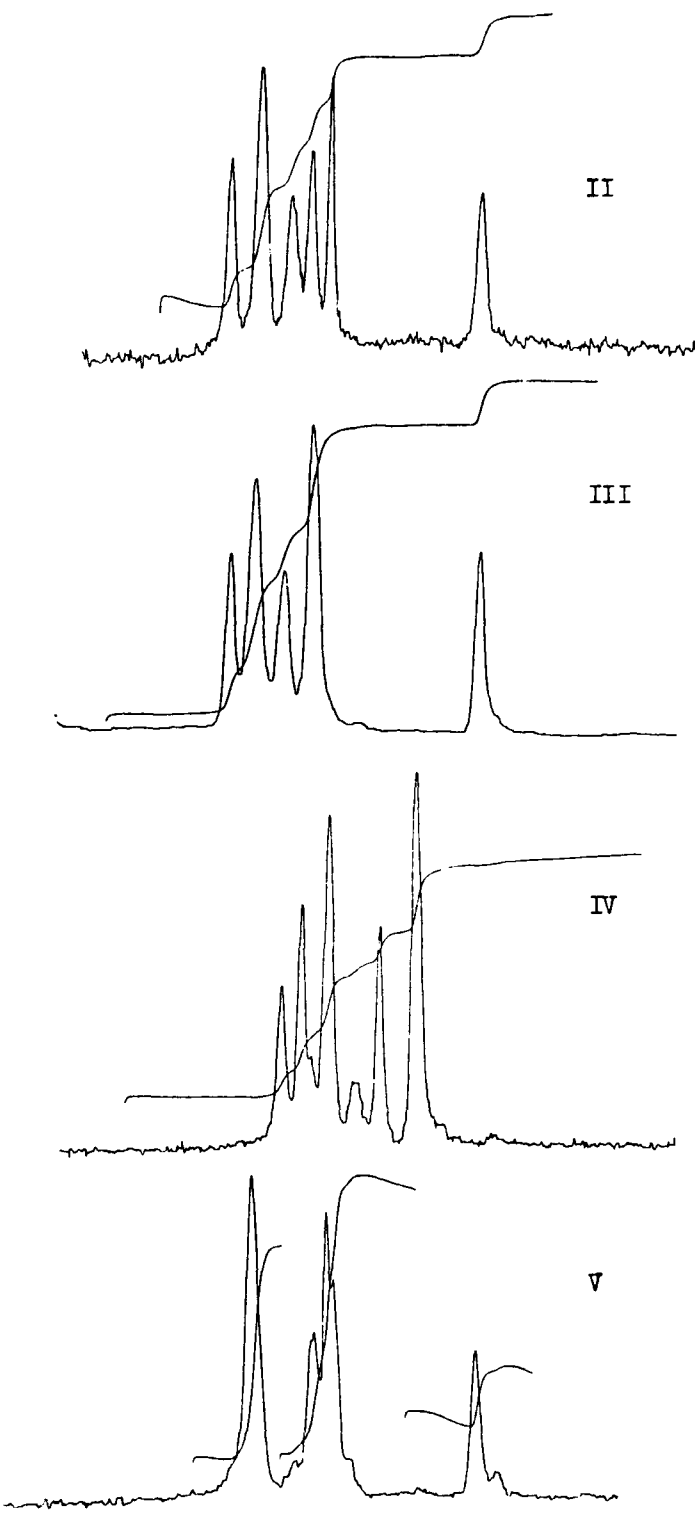


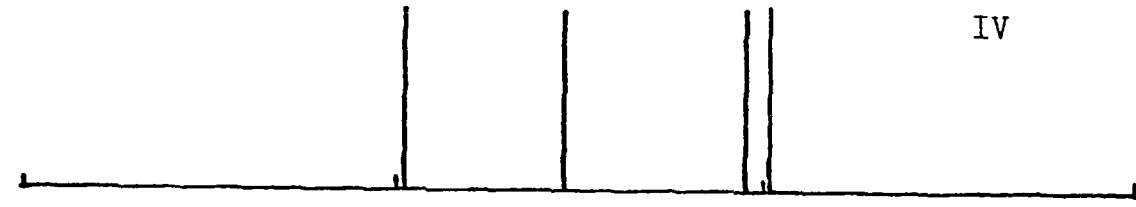
Fig. 4



II



III



IV



V

3 2 1 0

Chemical shift,  $\delta$ , in ppm

Fig. 5

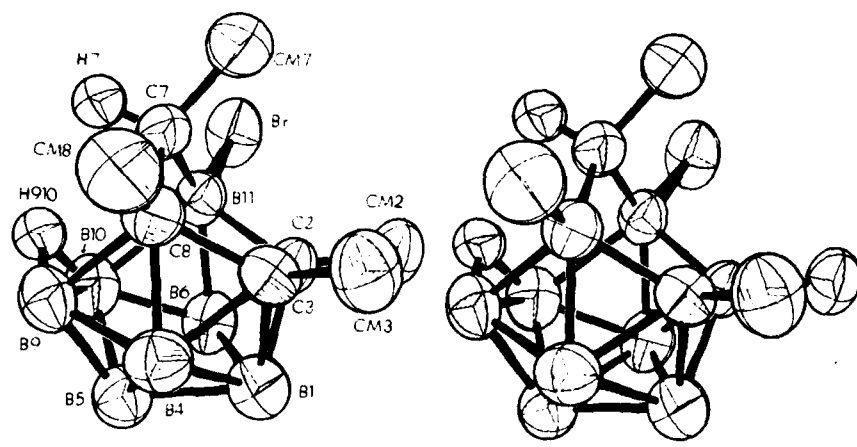


Fig. 6

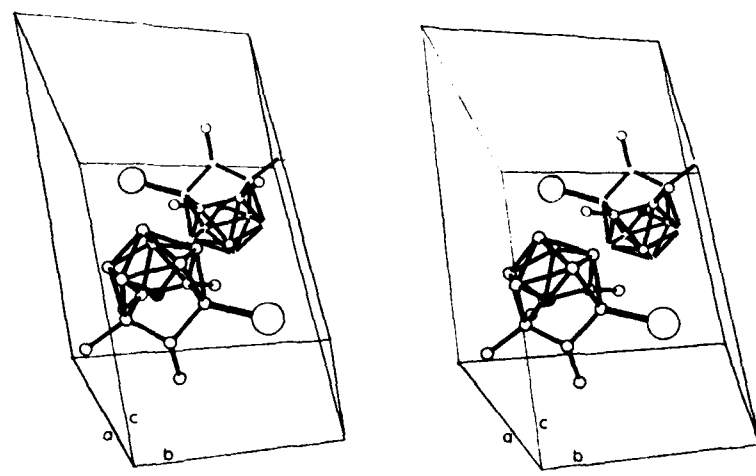
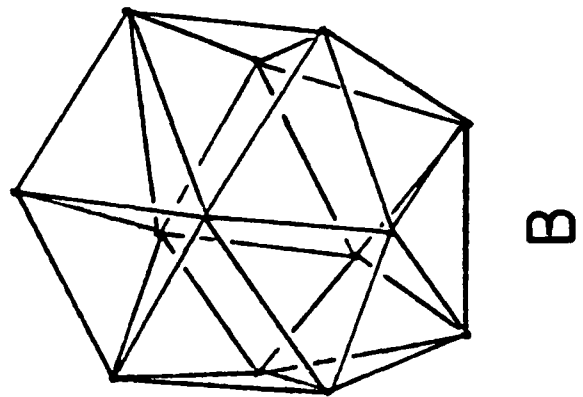
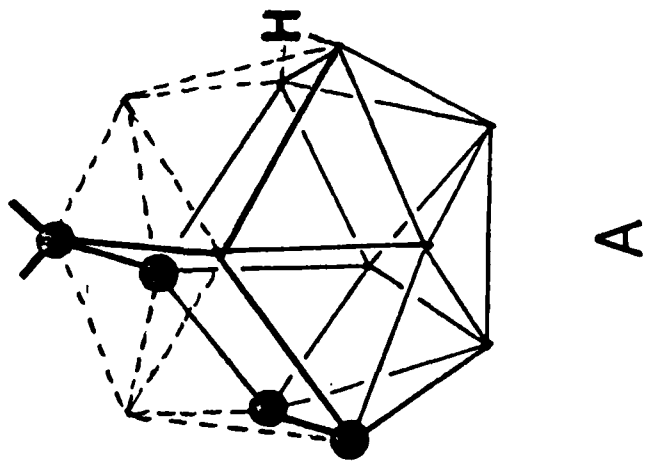


Fig. 7



B



A

Fig. 8

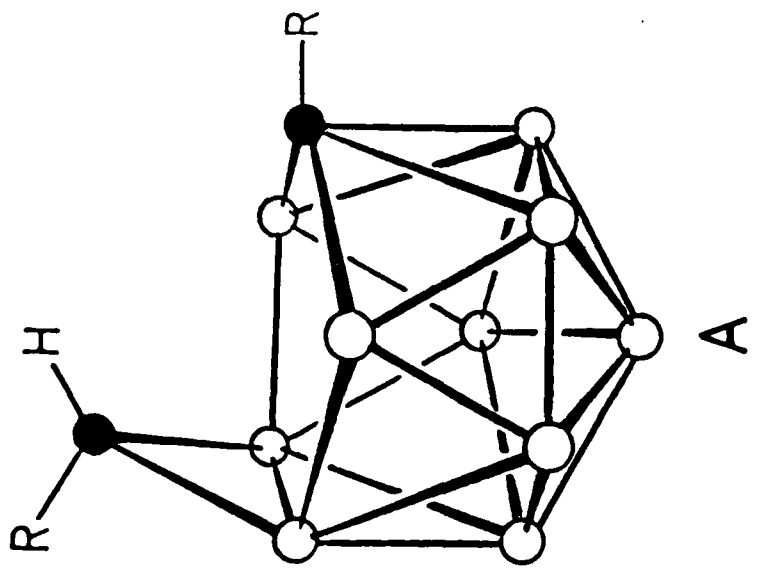
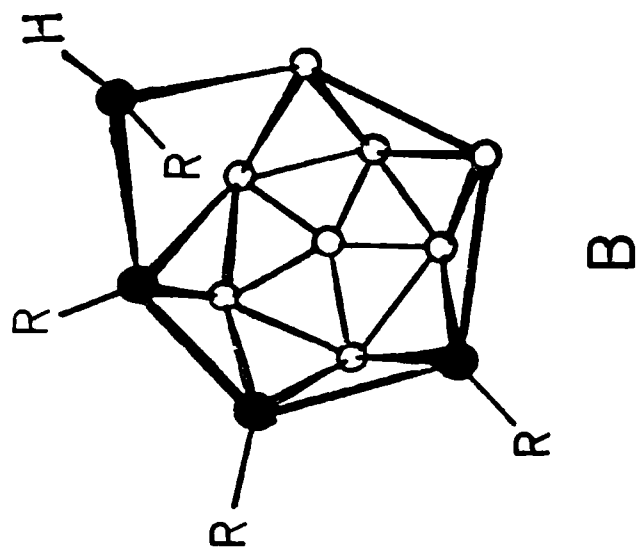


Figure 9

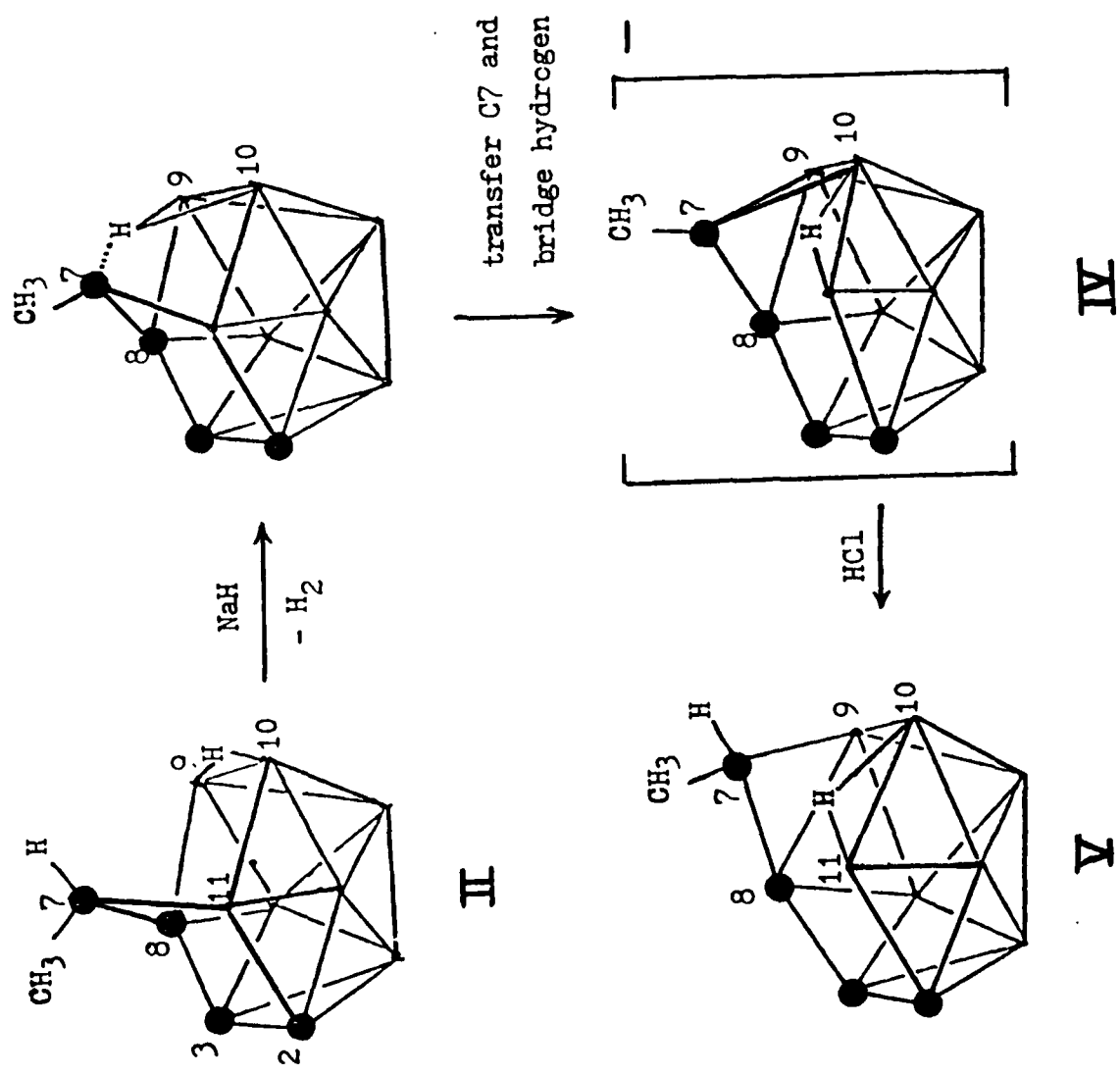
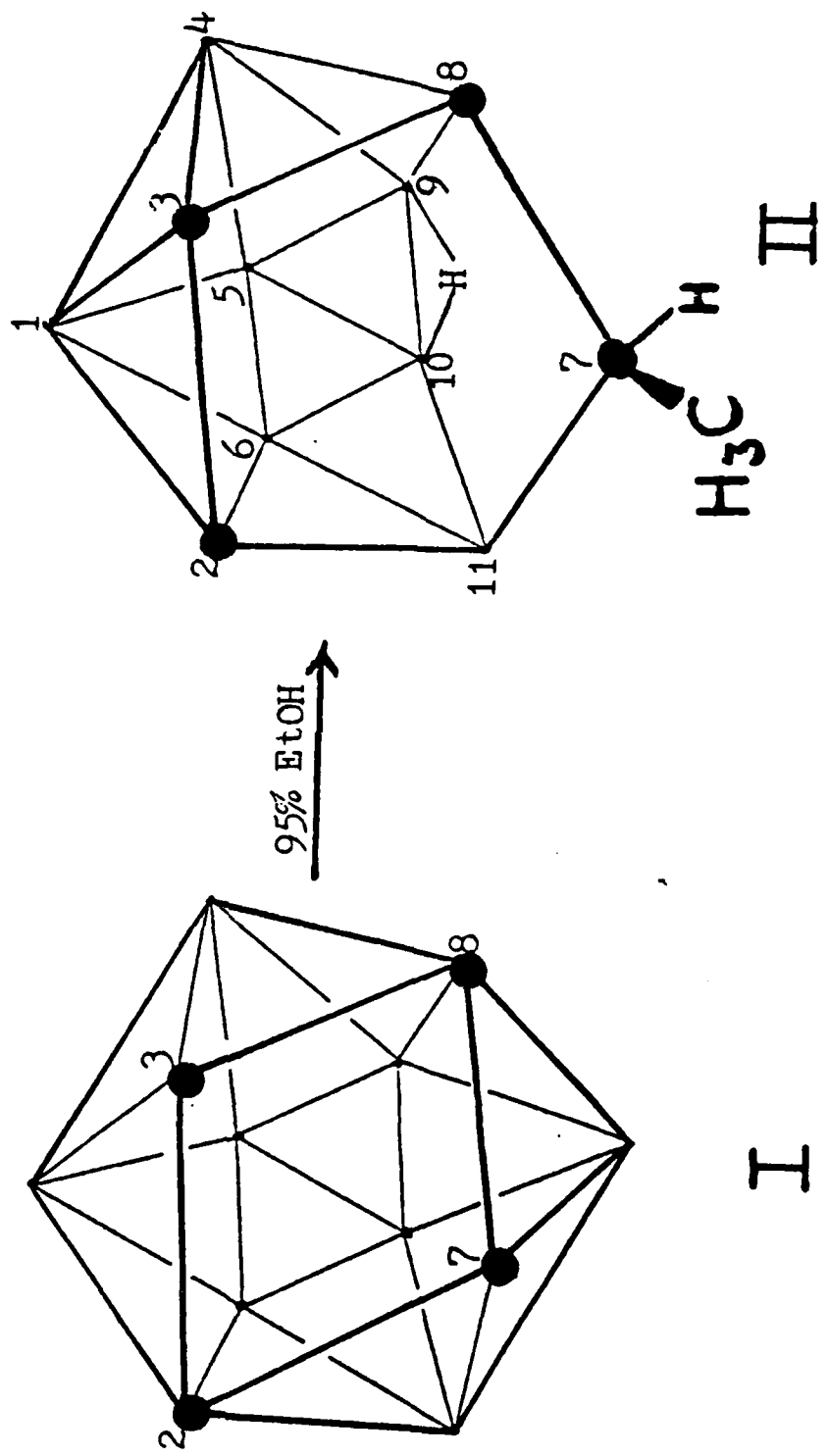


Fig. 10



## UNCLASSIFIED

SECURITY CLASSIFICATION OF THIS PAGE (When Data Entered)

REPORT DOCUMENTATION PAGE		READ INSTRUCTIONS BEFORE COMPLETING FORM
1. REPORT NUMBER Technical Report No. 37	2. GOVT ACCESSION NO. AD-Ac94338	3. FCIPIENT'S CATALOG NUMBER
4. TITLE (and Subtitle) Electron-Rich Carboranes. Studies of a Stereochemically Novel System. $(\text{CH}_3)_4\text{C}_4\text{B}_7\text{H}_9$ , an 11-Vertex Arachno Cluster		5. TYPE OF REPORT & PERIOD COVERED Interim
7. AUTHOR(s) David C. Finster and Russell N. Grimes		6. PERFORMING ORG. REPORT NUMBER N0001475-C-0305
8. PERFORMING ORGANIZATION NAME AND ADDRESS Department of Chemistry University of Virginia Charlottesville, Va. 22901		10. PROGRAM ELEMENT, PROJECT, TASK AREA & WORK UNIT NUMBERS Nr 053-569
11. CONTROLLING OFFICE NAME AND ADDRESS Chemistry Branch, Office of Naval Research Arlington, Virginia 22217		12. REPORT DATE January, 1981
14. MONITORING AGENCY NAME & ADDRESS (if different from Controlling Office)		13. NUMBER OF PAGES 43
16. DISTRIBUTION STATEMENT (of this Report)		15. SECURITY CLASS. (of this report) Unclassified
		15a. DECLASSIFICATION/DOWNGRADING SCHEDULE
17. DISTRIBUTION STATEMENT (of the abstract entered in Block 20, if different from report)		
18. SUPPLEMENTARY NOTES		
19. KEY WORDS (Continue on reverse side if necessary and identify by block number) Carborane Electron-rich carborane Tetracarbon carborane		
20. ABSTRACT (Continue on reverse side if necessary and identify by block number) See title page		

TECHNICAL REPORT DISTRIBUTION LIST, GEN

<u>No.</u>	<u>Copies</u>	<u>No.</u>	<u>Copies</u>
Office of Naval Research Attn: Code 472 800 North Quincy Street Arlington, Virginia 22217	2	U.S. Army Research Office Attn: CRD-AA-IP P.O. Box 1211 Research Triangle Park, N.C 27709	1
ONR Branch Office Attn: Dr. George Sandoz 536 S. Clark Street Chicago, Illinois 60605	1	Naval Ocean Systems Center Attn: Mr. Joe McCartney San Diego, California 92152	1
ONR Area Office Attn: Scientific Dept. 715 Broadway New York, New York 10003	1	Naval Weapons Center Attn: Dr. A. B. Amster, Chemistry Division China Lake, California 93555	1
ONR Western Regional Office 1030 East Green Street Pasadena, California 91106	1	Naval Civil Engineering Laboratory Attn: Dr. R. W. Drisko Port Hueneme, California 93401	1
ONR Eastern/Central Regional Office Attn: Dr. L. H. Peebles Building 114, Section D 666 Summer Street Boston, Massachusetts 02210	1	Department of Physics & Chemistry Naval Postgraduate School Monterey, California 93940	1
Director, Naval Research Laboratory Attn: Code 6100 Washington, D.C. 20390	1	Dr. A. L. Slafkosky Scientific Advisor Commandant of the Marine Corps (Code RD-1) Washington, D.C. 20380	1
The Assistant Secretary of the Navy (RE&S) Department of the Navy Room 4E736, Pentagon Washington, D.C. 20350	1	Office of Naval Research Attn: Dr. Richard S. Miller 800 N. Quincy Street Arlington, Virginia 22217	1
Commander, Naval Air Systems Command Attn: Code 310C (H. Rosenwasser) Department of the Navy Washington, D.C. 20360	1	Naval Ship Research and Development Center Attn: Dr. G. Bosmajian, Applied Chemistry Division Annapolis, Maryland 21401	1
Defense Technical Information Center Building 5, Cameron Station Alexandria, Virginia 22314	12	Naval Ocean Systems Center Attn: Dr. S. Yamamoto, Marine Sciences Division San Diego, California 91232	1
Dr. Fred Saalfeld Chemistry Division, Code 6100 Naval Research Laboratory Washington, D.C. 20375	1	Mr. John Boyle Materials Branch Naval Ship Engineering Center Philadelphia, Pennsylvania 19112	1
Professor M. Newcomb Texas A&M University Department of Chemistry College Station, Texas 77843	1	Professor Richard Eisenberg Department of Chemistry University of Rochester Rochester, New York 14627	1

TECHNICAL REPORT DISTRIBUTION LIST, 053

<u>No.</u>	<u>Copies</u>	<u>No.</u>	<u>Copies</u>
		Professor H. Abrahamson	
		Department of Chemistry	
		University of Oklahoma	
		Norman, Oklahoma 73019	1
Dr. M. F. Hawthorne Department of Chemistry University of California Los Angeles, California 90024	1	Dr. M. H. Chisholm Department of Chemistry Indiana University Bloomington, Indiana 47401	1
Dr. D. B. Brown Department of Chemistry University of Vermont Burlington, Vermont 05401	1	Dr. B. Foxman Department of Chemistry Brandeis University Waltham, Massachusetts 02154	1
Dr. W. B. Fox Chemistry Division Naval Research Laboratory Code 6130 Washington, D.C. 20375	1	Dr. T. Marks Department of Chemistry Northwestern University Evanston, Illinois 60201	1
Dr. J. Adcock Department of Chemistry University of Tennessee Knoxville, Tennessee 37916	1	Dr. G. Geoffrey Department of Chemistry Pennsylvania State University University Park, Pennsylvania 16802	1
Dr. A. Cowley Department of Chemistry University of Texas Austin, Texas 78712	1	Dr. J. Zuckerman Department of Chemistry University of Oklahoma Norman, Oklahoma 73019	1
Dr. W. Hatfield Department of Chemistry University of North Carolina Chapel Hill, North Carolina 27514	1	Professor O. T. Beachle, Department of Chemistry State University of New York Buffalo, New York 14214	1
Dr. D. Seyferth Department of Chemistry Massachusetts Institute of Technology Cambridge, Massachusetts 02139	1	Professor P. S. Skell Department of Chemistry The Pennsylvania State University University Park, Pennsylvania 16802	1
Professor Ralph Rudolph Department of Chemistry University of Michigan Ann Arbor, Michigan 48109	1	Professor K. M. Nicholas Department of Chemistry Boston College Chestnut Hill, Massachusetts 02167	1
Mr. James Kelley DTNSRDC Code 2803 Annapolis, Maryland 21402	1	Professor R. Neilson Department of Chemistry Texas Christian University Fort Worth, Texas 76129	1
		Dr. Rudolph J. Marcus Office of Naval Research Scientific Liaison Group American Embassy APO San Francisco 96503	1

DATE  
ILMED  
- 8